

# *Research on Thermal Deformation Behavior of GH696 Superalloys*

**Haozhou Gou, Chuanzhi Zhu, Mingrong Yuan, Kaibin Fan, Ning Liu, Bin Liu**

*AECC Aviation Power Co., Ltd., Precision Forging Center, Xi'an, 710021, China*

**Keywords:** GH696 superalloy, Thermal deformation behavior, Mechanical behavior, Thermal processing map

**Abstract:** In this study, the mechanical behavior of GH696 alloy during high temperature compression deformation were studied on the Gleeble-3500. Based on the results of thermal simulation compression deformation experiment, the thermal processing maps of the alloy were drawn. The results show that the flow stress of GH696 alloy during thermal simulated compression deformation decreases with the increase of deformation temperature and increases with the increase of strain rate. The dynamic softening effect of GH696 alloy is small, and the flow stress reaches the peak flow stress and enters the steady flow stage. The strain rate sensitivity index of GH696 alloy increases with the increase of deformation temperature and decreases with the increase of strain rate. The strain hardening index of GH696 alloy decreases with the increase of deformation temperature and increases with the increase of strain rate. It provides a theoretical basis for the regulation of GH696 alloy precision forging process.

## **1. Introduction**

GH696 alloy is an iron-based deformation superalloy that can withstand working temperatures ranging from 400 °C to 700 °C. Compared to nickel-based superalloys, it has a lower cost and better thermal processing performance, making it suitable for use in rods, wires, plates, and strips [1-3]. GH696 alloy is an age-hardening superalloy composed of stable austenite made up of Fe, Ni, and Cr with the addition of 1.4wt% Mo to strengthen the solid solution and an appropriate amount of B to strengthen the grain boundary. The high Ti/Al ratio in GH696 alloy allows for precipitation hardening through the formation of Ti-rich metastable phase (Ni<sub>3</sub>AlTi) [4, 5].

The high temperature deformation process parameters exhibit a close correlation with the microstructure and mechanical properties, ensuring the quality of forging. These parameters include pre-heating temperature, starting and ending deformation temperatures, degree of deformation, deformation speed, etc. The selection of high temperature deformation process parameters for superalloys is relatively intricate and primarily relies on qualitative analysis. Henceforth, it becomes imperative to systematically investigate the impact of high temperature deformation processes on the microstructure and mechanical properties of superalloys while quantitatively describing their behavior during such conditions. Consequently, studying the mechanical behavior of GH696 alloy during high temperature deformation can provide a theoretical foundation for regulating its precision forging process.

## 2. Experimental procedures

The experimental material used in this study is a GH696 alloy bar with a diameter of 60 mm. Its chemical composition is shown in Table 1, and its original microstructure is shown in Figure 1. It is evident from Figure 1 that the GH696 alloy possesses equiaxed austenitic grains with an average grain size of approximately 15  $\mu\text{m}$ .

Table 1: Chemical composition of GH696 alloy (wt%)

Cr	Ni	Mo	Ti	Al	Mn	Fe
10.0-12.5	21.0-25.0	1.0-1.6	2.6-3.2	$\leq 0.8$	$\leq 0.6$	Bal.

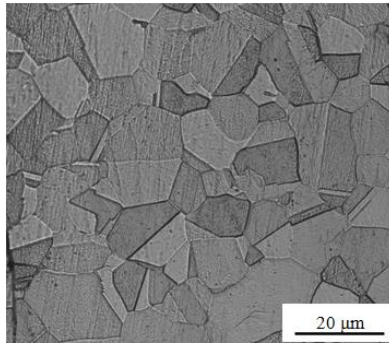


Figure 1: Microstructure of supplied GH696 alloy

The thermal compression deformation test of GH696 alloy was conducted on the Gleeble-3500 thermal simulation test machine, utilizing cylindrical compression samples with a diameter of 8 and a length of 12 mm. During the experiment, the sample was initially heated to the desired deformation temperature at a heating rate of 10  $^{\circ}\text{C}/\text{s}$ , followed by a dwell time of 5 minutes before being subjected to compression at a constant strain rate. Subsequently, rapid water-cooling was employed to bring the sample back to room temperature. The deformation temperatures investigated were 880  $^{\circ}\text{C}$ , 910  $^{\circ}\text{C}$ , 940  $^{\circ}\text{C}$ , 970  $^{\circ}\text{C}$ , 1000  $^{\circ}\text{C}$ , 1030  $^{\circ}\text{C}$ , 1060  $^{\circ}\text{C}$ , 1090  $^{\circ}\text{C}$  and 1120  $^{\circ}\text{C}$  respectively. The strain rates applied were set as follows: 0.01  $\text{s}^{-1}$ , 0.1  $\text{s}^{-1}$ , 1.0  $\text{s}^{-1}$  and 10  $\text{s}^{-1}$ , while the levels of deformation amounted to 30 %, 40 %, 50 % and 60 %.

Following the thermal simulation compression deformation experiment of GH696 alloy, the deformed alloy was sectioned along the axis of the compression sample and one half of it was utilized for preparing a metallographic sample. Optical metallographic observation was conducted using Leica-DMI 3000M inverted metallographic microscope.

## 3. Results and discussions

### 3.1 Mechanical behavior of thermal deformation

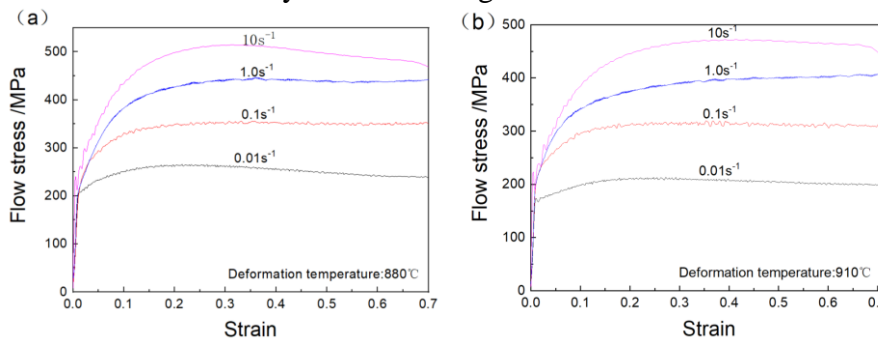
Fig. 2 is the stress-strain curve in the heat simulation compression deformation process for GH696 alloy. The flow stress of the alloy in the initial stage of the heat simulation compression deformation was increased dramatically with the increase of strain. The increase of the flow stress of the alloy is basically stable after the peak flow stress goes forward and the steady flow phase of the stable flow phase. In the early stage of heat simulation compression deformation, the deformation of the error density is rapidly increased, and the process of processing sclerosis occurs, and the continuous deformation time dislocation is caused by the slip, and the softening effect caused by the sliding movement is not sufficient to offset the hardening effect of the dislocation density, so the stress increases sharply with the increase of strain. As the strain continues to increase,

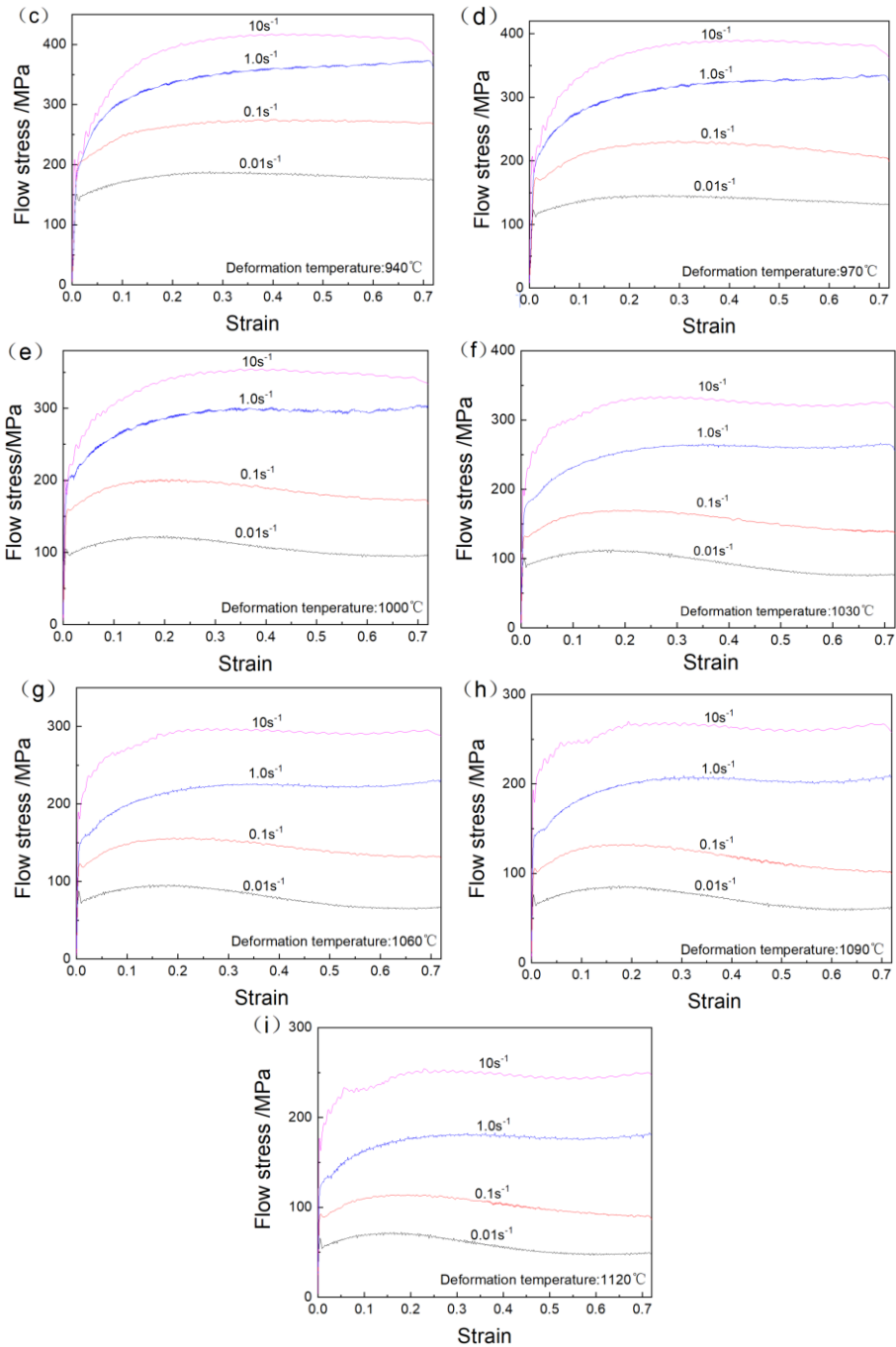
the processing hardening effect of dislocation propagation is balanced by the dislocation of the different dislocation, the offset and the dislocation of the dislocation, so the flow stress of the GH696 alloy is the same as the flow stress of the peak flow stress in the steady state flow phase.

When the deformation temperature is constant, the flow stress of GH696 alloy increases obviously with the increase of strain rate. This is because when the strain rate increases, the dislocation proliferation rate increases and the equilibrium dislocation density increases during the thermal simulation compression deformation process, which leads to the strengthening of the work hardening effect. Meanwhile, the time required to reach the same deformation degree decreases, and the softening effect caused by dislocation slip and climb decreases, which cannot offset the work hardening effect caused by the increase in strain rate. Therefore, the flow stress of GH696 alloy increases.

When the strain rate is constant, the flow stress of GH696 alloy decreases with the increase of deformation temperature. There are two reasons for this phenomenon, GH696 alloy is a precipitation-hardened superalloy, which contains a lot of strengthened phase particles. With the increase of deformation temperature, the strengthened phase particles gradually dissolve, and the hindering effect on dislocation movement becomes weaker during thermal simulation compression deformation, so the flow stress of GH696 alloy decreases. On the other hand, when the deformation temperature increases, the thermal activation effect is enhanced, the average free energy of atoms is increased, the ability to overcome the energy barrier is enhanced, the ability to overcome the obstruction during dislocation movement is enhanced, and the flow stress of GH696 alloy is reduced.

When the strain rate is  $0.01 \text{ s}^{-1}$  and  $0.1 \text{ s}^{-1}$  and the deformation temperature is  $880\text{-}940 \text{ }^{\circ}\text{C}$ , the flow stress of GH696 alloy increases rapidly and enters the steady flow stage. When the deformation temperature is  $1000\text{-}1120 \text{ }^{\circ}\text{C}$ , the flow stress of GH696 alloy reaches the maximum value and gradually decreases with the increase of strain, that is, it enters the softening stage. This is because when the deformation temperature is higher, the thermal activation effect is enhanced, the average free energy of atoms is increased, the motion ability is enhanced, and the obstacle overcoming ability during dislocation movement is enhanced. When the strain rate is  $1.0 \text{ s}^{-1}$ , the stress of GH696 alloy increases rapidly and then enters a slow increase stage at low deformation temperature ( $910\text{-}970 \text{ }^{\circ}\text{C}$ ), while it directly enters a steady flow stage at high deformation temperature ( $1000\text{-}1120 \text{ }^{\circ}\text{C}$ ). This may be due to the larger strain rate, faster dislocation proliferation rate, larger work hardening degree, lower deformation temperature and less obvious softening effect. Under the combined effect of these two reasons, the work hardening effect is always in a dominant position, so the flow stress of GH696 alloy continues to increase. When the strain rate is  $10.0 \text{ s}^{-1}$ , the flow stress of GH696 alloy reaches the maximum and enters the steady flow stage. However, the softening effect cannot exceed the hardening effect, but reaches an equilibrium state and enters the steady-state flow stage.





a: 880 °C, b: 910 °C, c: 940 °C, d: 970 °C, e: 1000 °C, f: 1030 °C, g: 1060 °C, h: 1090 °C, i: 1120 °C

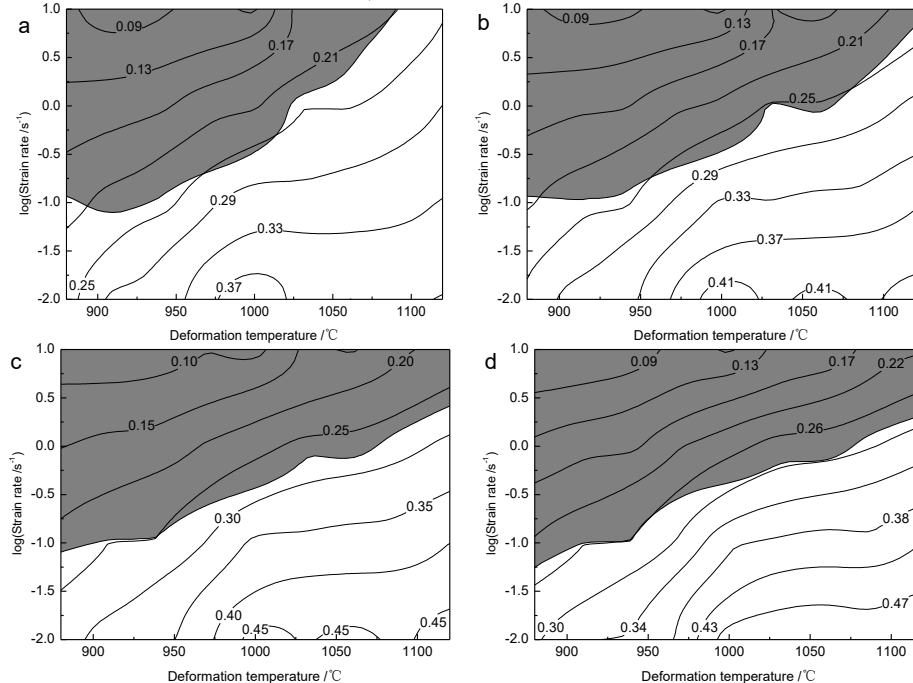
Figure 2: Stress-strain curve of GH696 alloy during thermal simulated compression deformation

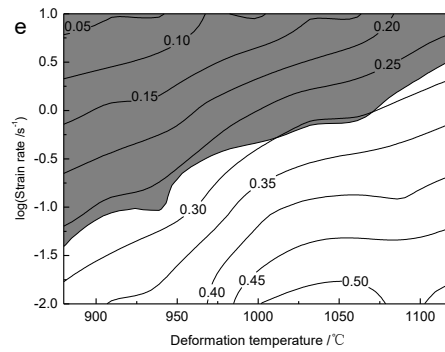
### 3.2 Thermal processing map

Based on the experimental results of thermal simulation compression deformation of GH696 alloy, the thermal processing map of GH696 alloy under thermal simulation compression deformation under different strains was established, as shown in Fig. 3, where the value on the isoline is the value of energy dissipation rate, and the shaded area represents the plastic instability region when the stability function is negative. It can be seen from Fig. 3 that the energy dissipation

rate curve of GH696 alloy under thermal simulated compression deformation under various strains is relatively straight and increases with the increase of deformation temperature and the decrease of strain rate. The energy dissipation rate of GH696 alloy during thermal simulation compression deformation changes obviously with deformation temperature, but changes little with strain rate. It can be seen from Fig. 3(c)-(d) that when the strain rate is  $2.0-10.0 \text{ s}^{-1}$ , the GH696 alloy is in the unstable region in the whole experimental deformation temperature range, so the appropriate strain rate should be selected.

As can be seen from Fig. 3, strain has little influence on the thermal working diagram of GH696 alloy during thermal simulated compression deformation. When the strain is 0.2, the non-stable region of GH696 alloy is mainly in the region of deformation temperature of  $880-970 \text{ }^\circ\text{C}$  and strain rate of  $0.01-10.0 \text{ s}^{-1}$  and the region of deformation temperature of  $970-1090 \text{ }^\circ\text{C}$  and strain rate of  $1.0-10.0 \text{ s}^{-1}$ . When the strains are 0.3, 0.4, 0.5 and 0.6, the non-stable region of GH696 alloy during thermal simulation compression deformation mainly occurs in the region of deformation temperature of  $880-1000 \text{ }^\circ\text{C}$  and strain rate of  $0.1-10.0 \text{ s}^{-1}$  and the region of deformation temperature of  $1000-1120 \text{ }^\circ\text{C}$  and strain rate of  $0.1-10.0 \text{ s}^{-1}$ . In addition, the peak energy dissipation rates of GH696 alloy during thermal simulated compression deformation are 0.41, 0.41, 0.45, 0.51 and 0.55, respectively, when the strain is 0.2-0.6. When the strain is 0.2, the peak energy dissipation rate of GH696 alloy is  $970-1030 \text{ }^\circ\text{C}$ , and the strain rate is  $0.01 \text{ s}^{-1}$ . When the strain is 0.3 and 0.4, the peak energy dissipation rate corresponding to the deformation temperature of GH696 alloy is  $1000 \text{ }^\circ\text{C}$ ,  $1060 \text{ }^\circ\text{C}$  and  $1120 \text{ }^\circ\text{C}$ , and the strain rate is  $0.01 \text{ s}^{-1}$ . When the strain is 0.5, the peak energy dissipation rate of GH696 alloy during thermal simulated compression deformation corresponds to the deformation temperature of  $1000-1120 \text{ }^\circ\text{C}$  and the strain rate is  $0.01 \text{ s}^{-1}$ . When the strain is 0.6, the peak energy dissipation rate of GH696 alloy corresponds to the deformation temperature of  $1000-1060 \text{ }^\circ\text{C}$  and  $1120 \text{ }^\circ\text{C}$ , and the strain rate is  $0.01 \text{ s}^{-1}$ .





a:  $\varepsilon=0.2$ , b:  $\varepsilon=0.3$ , c:  $\varepsilon=0.4$ , d:  $\varepsilon=0.5$ , e:  $\varepsilon=0.6$

Figure 3: Thermal processing diagram of GH696 alloy during thermal simulated compression deformation

#### 4. Conclusions

The mechanical behavior of GH696 alloy during high temperature compression deformation were studied based on the experimental results of thermal simulation. The flow stress of GH696 alloy during thermal simulated compression deformation decreases with the increase of deformation temperature and increases with the increase of strain rate. The dynamic softening effect of GH696 alloy is small, and the flow stress reaches the peak flow stress and enters the steady flow stage. The strain rate sensitivity index of GH696 alloy increases with the increase of deformation temperature and decreases with the increase of strain rate. The strain hardening index of GH696 alloy decreases with the increase of deformation temperature and increases with the increase of strain rate.

#### References

- [1] Zhaohua Xu, Miaoquan Li, Hong Li. Plastic flow behavior of superalloy GH696 during hot deformation [J]. *Transactions of Nonferrous Metals Society of China*, 2016. DOI: 10.1016/S1003-6326(16)64161-4.
- [2] Xiaoling H. A Trial Production of Alloy GH696 with Experimental Analysis [J]. *Research on Iron and Steel*, 2002.
- [3] Xu Z H, Li H, Li M Q. Dynamic recrystallization model of GH696 superalloy [J]. *Chinese Journal of Nonferrous Metals*, 2017, 27(8):1551-1562. DOI:10.19476/j.ysxb.1004.0609.2017.08.03.
- [4] Jiangbo Z, Center T. Research on Measures to Improve Mechanical Properties of GH696 Cold Rolled Sheet [J]. *Special Steel Technology*, 2014.
- [5] Yuchen W, Guilin Wu, Changhong Z, et al. Effect of Secondary Age Treatment on Mechanical Properties and Microstructure of GH696 Alloy [J]. *Journal of Iron and Steel Research*, 2011.